Synchronisation and relative position of airborne bistatic radar

Matthias Weiß
Forschungsgesellschaft für Angewandte Naturwissenschaften-FHR
Neuenahrer Strasse 20
D 53343 Wachtberg, Germany

weiss@fgan.de

ABSTRACT

The interest in bi- and multistatic radar has been growing over the last years as they offer various advantages. For instance the transmitter and receiver can be easily be separated and therefore the survivability can be enhanced by deploying the transmitter further away from the scene. Even the possibility of a forward looking synthetic aperture radar can be realised. Bistatic radar can provide a cost effective solution as the transmitter and receiver can be build without the cost driven transmit/receive-modules. Beyond this, with large baselines it is likely to increase the signature from stealthy objects. Another interesting aspect of bistatic imaging radar is the reduced dynamic range of difficult imaging environments such as urban ones.
However, besides the benefits of bi- and multistatic radar one has to solve several technical problems [3] - such as the synchronisation of the stable local oscillators (STALO), the involved automatic adjustment of transmit pulse versus receive gate timing, antenna pointing and flight coordination. For a highly automatic bistatic signal processing, the baseline between the involved platforms, as well as the orientation towards each other must be known precisely besides. This paper discusses a method which allows determining these two fundamental parameters of an airborne bi-/multistatic SAR system.

1 INTRODUCTION

Over the past years the interest in bi- and multistatic radar is increasing steadily as the technology has improved dramatically in comparison to the early trials in past century. Benefits of bi- and multistatic radar can be found in survivability of the platforms, as the receiver is passive and the transmitter can be deployed further away from the scene, or even replace the single transmitter by multiple low-cost transmitters on UAVs. Using a bistatic setup for imaging radars enables a forward looking mode, which is not attainable for monostatic SAR systems. Bi- and multistatic radar allows to achieve a cost effective surveillance of an area of interest due to its possible covert surveillance and economic spectrum occupancy. Beyond this, with large baselines it is likely to increase the signature from stealthy objects. Another interesting aspect of bistatic imaging radar is the reduced dynamic range of difficult imaging environments such as urban ones.

In recent years the requirement on bi- and multistatic radar systems has increased steadily. Directly associated with these requirements, one has to solve the problem of highly accurate time and frequency synchronisation for coherent signal processing [1], [2] and localisation. If moving platforms are involved,

Weiß, M. (2006) Synchronisation and Relative Position of Airborne Bistatic Radar. In *Bistatic-Multistatic Radar and Sonar Systems* (pp. 20-1 – 20-10). Meeting Proceedings RTO-MP-SET-095, Paper 20. Neuilly-sur-Seine, France: RTO. Available from: http://www.rto.nato.int/abstracts.asp.

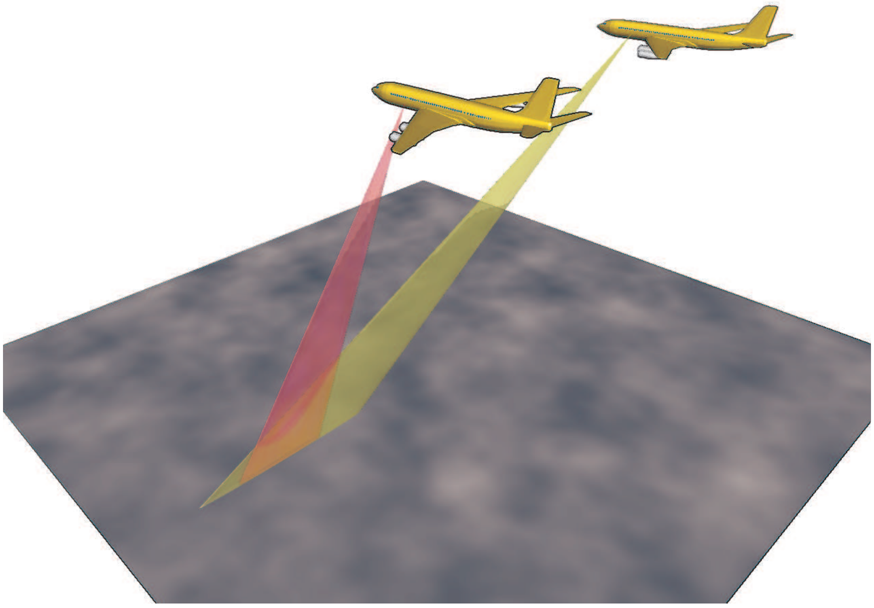

Figure 1: Two airborne SAR platforms composing a bistatic SAR system

as in the case of synthetic aperture radar (SAR) (see Fig. 1), high precision navigation is an issue for motion compensation and for alignment of the antenna footprints on ground. For a high degree of automation of bi-/multistatic imaging data processing the baseline between transmitter and receiver and the orientation of the platform towards each other must be known precisely during the recording. These parameters directly affect the achievable geometrical resolution and the geometry of the radar system.

Up to now, these crucial parameters of a bi-/multistatic imaging radar system, baseline and orientation, are determined using a Global Navigation Satellite System (GNSS) - like the GPS - and differential GNSS systems (for instance DGPS) receivers on each involved platform. The typical accuracy of a DGPS in real-time is about 10 cm and several millimeters after post-processing (see Fig. 2). For a high resolution bistatic imaging radar the demanded real-time accuracy is in the range of millimeters. Higher efforts at the baseline measurement, with typical 0.3 mm accuracy, are needed for interferometric X-band SAR systems.

The requirements on bistatic imaging radar systems increase continuously in common with the performance increase on monostatic radar. However, besides the processing of the bistatic radar data one has to solve several technical problems [3] [4] - such as the synchronisation of the stable local oscillators (STALO), the involved automatic adjustment of transmit pulse versus receive gate timing, antenna pointing and flight coordination. For a highly automatic bistatic signal processing of imaging radar, the baseline between the involved platforms, as well as the orientation towards each other must be known precisely. This paper will discuss a method which allows determining these two fundamental parameters of an airborne bi-/multistatic SAR system.

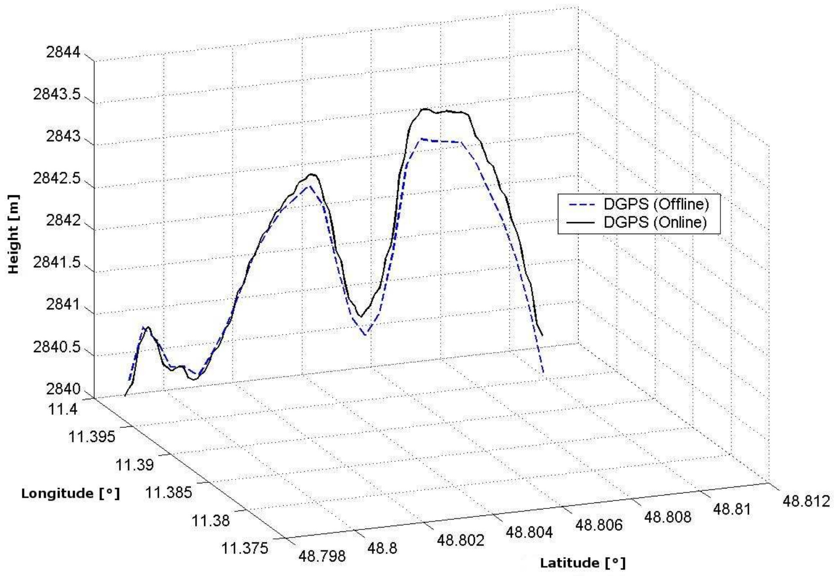

Figure 2: Comparison between two DGPS tracks (online and offline processing)

2 Setup

For a bi-/multistatic radar system one has to solve the problems of synchronisation and precision navigation. If the involved platforms are airborne or space-based the orientation towards each other has to be determined in real time to align the antenna footprints at the interesting scene. Fig. 1 shows a typical airborne bistatic SAR configuration.

Concurrent with the precision navigation, which is essential for hight accuracy determination of the baseline, the time has to be transferred from the transmitter platform to the receiver platform. Several publications ([5], [6]) suggest to transfer a calibration signal from the TX platform to the RX platform und vice-versa. This proposed solution has two main drawbacks. The first one is that a calibration signal has to be generated on all participating platforms und has to be transferred to all other platforms. Due to this, no passive receiver exists and the whole system can easily be detected. The second shortcoming is that the determination of the baseline and time correction can only take place during post-processing. If these parameters were already known at the measurement, it would be possible to adjust the receiving time gate and align the antenna footprints. Consequentially time consuming data optimization steps can be avoided.

To overcome this problem we propose the following approach. A dedicated navigation unit will be installed on the transmitter and one on the receiver platform. On the transmitter platform the navigation unit will create a signal from the stable local oscillator. This signal will be split into four individual navigation signals. These four channels are modulated, each one with a unique binary pseudo-random noise (PRN) sequence for ranging and an additional navigation (broadcast) message. Each of these navigation signals is transmitted over separate antennas, which are distributed over the transmitter platform. A block diagram of the navigation unit on the transmitter platform is shown in Fig. 3. The navigation antennas are aligned towards the RX platform. The arrangement of the antennas on the TX platform must be done in such a manner that a maximum face is spanned toward the RX platform.

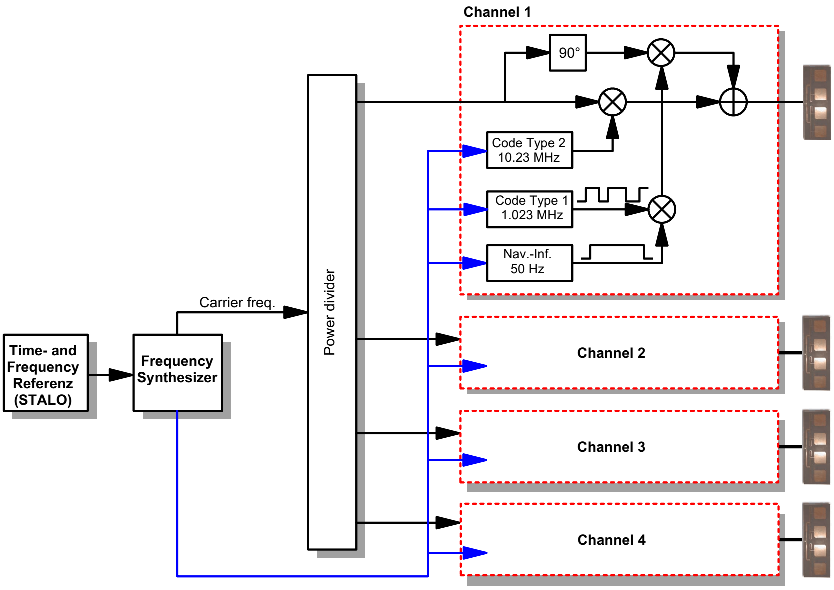

Figure 3: Block diagram of the navigation unit on the transmitter platform, generating four individual navigation signals

For ranging information each of the navigation signal is modulated by one of several codes, for instance with a 1 millisecond long acquisition signal with a chipping rate of 1.023 MHz. An additional (broadcast) message, which is likewise modulated onto each navigation signal, includes information about the navigation antenna configuration on the transmitter platform (e.g. offset from the primary TX antenna, GPS coordinates, heading, and calibration terms). The PRN codes are chosen from a set of Gold codes and are unique for each navigation signal. Hence, the correlation between any pair of codes is very low. This allows using the same carrier frequency for all navigation signals. The four navigation signals are transmitted using separate navigation antennas and therefore possess a slightly different travel path to a receiver unit. This circumstance is shown in Fig. 4 where four different navigation signals travels from the TX platform to a single navigation antenna on the RX platform. Due to this circumstance the four navigation signals arrives with unequal time delays at the same point on the receiver side.

On the RX platform there are likewise four navigation antennas installed. As on the transmitter platform these navigation antennas are distributed over the receiver platform in a manner that a maximum area is spanned toward the other platform. Fig. 5 illustrates the possible combination of travel paths from the TX to the RX platform for the navigation signals. Every navigation antenna on the RX platform feeds a receiver unit. The received signals are amplified, down-converted and digitized. For coherent signal processing all local frequencies of all four navigation units are generated from the local stable oscillator.

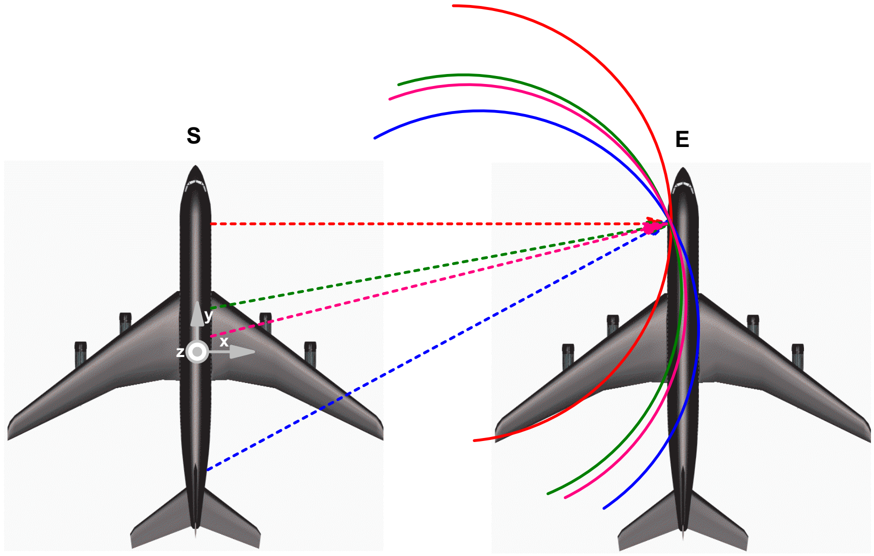

Figure 4: Two SAR platforms and the paths of four navigation signals arriving at one point on the receiver platform

3 Processing

The processing of the digitized signal is done in several blocks and can be roughly divided into the following steps. The block diagram of a receiver unit is shown in Fig. 6. To ensure a maximum of coherent signal processing all navigation units are driven by the same local stable oscillator.

The first step of processing is to search for the known PRN sequences of the four navigation signals in parallel. After detecting the codes a tracking takes over of the code and carrier phase.

To extract the (broadcast) message out of the navigation signal a bit synchronisation is performed. After frame synchronisation the message can be decoded and the required calibration terms will be extracted for further calculations. The (broadcast) message contains information about the position and heading of the TX platform (point of origin of the TX navigation antennas is on the TX platform), and the correction terms for four navigation signals, for instance.

The distance between the TX navigation antennas and the RX navigation antennas can be determined by the time of the signal propagations $r = c\,(t_{RX} - t_{TX}) = c\,\Delta t$, with the time stamp from the transmitter t_{TX} and from the receiver t_{RX}. The *measured distance* R_{ij} between the TX and RX (the pseudorange) is influenced by the lack of time synchronization between the clocks on the TX platform and the RX platform (ΔT). Other bias effects include multipath and receiver noise are taken into account by ϵ_{ij}.

$$R_{ij} = c(t_{RX} - t_{TX} + \Delta T + \epsilon_{ij}) \quad (1)$$
$$R_{ij} = r_{ij} + c(\Delta T + \epsilon_{ij}) \quad (2)$$

The indices i denotes the transmitter antenna, j the receiver antenna and c is the speed of light. For further

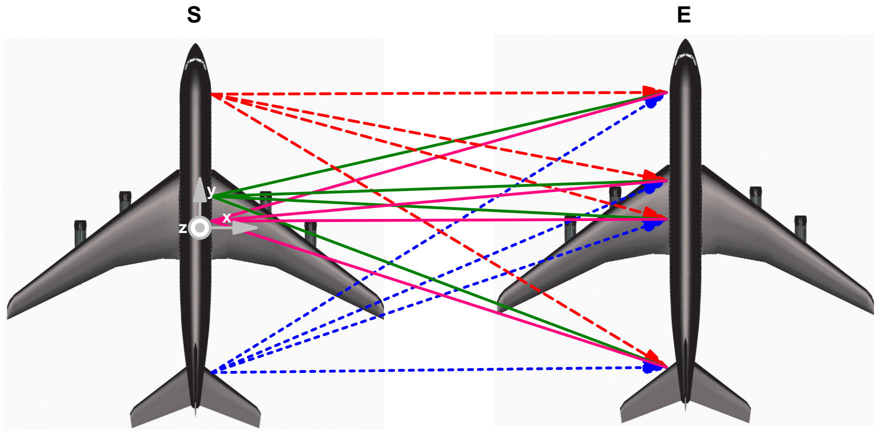

Figure 5: Two SAR platforms and the possible combination of navigation signals on the RX platform

calculation the time difference between the local clocks ΔT and ϵ_{ij} can be combined to a single variable as noise and multipath effects are for all receiving navigation signal nearly identical.

As four navigation signals are transmitted from the TX platform toward the RX platform it is possible to formulate four pseudorange equations for each navigation receiver:

$$(x_1-u_{xj})^2+(y_1-u_{yj})^2+(z_1-u_{zj})^2 = (R_{1j}-c\,\Delta T)^2 \quad (3)$$
$$(x_2-u_{xj})^2+(y_2-u_{yj})^2+(z_2-u_{zj})^2 = (R_{2j}-c\,\Delta T)^2 \quad (4)$$
$$(x_3-u_{xj})^2+(y_3-u_{yj})^2+(z_3-u_{zj})^2 = (R_{3j}-c\,\Delta T)^2 \quad (5)$$
$$(x_4-u_{xj})^2+(y_4-u_{yj})^2+(z_4-u_{zj})^2 = (R_{4j}-c\,\Delta T)^2 \quad (6)$$

with x_i, y_i, z_i the known position of the navigation antenna i on the TX platform (i = 1,2,3,4) and u_{xj}, u_{yj}, u_{zj} the position of the navigation antenna j on the receiver platform. R_{ij} is the measured distance between the navigation antenna on the TX platform i and the RX platform j. The point of origin for all measurements is on centered on the TX platform. The range error introduced by the time difference between both platforms is described by $c\,\Delta T$. This nonlinear equation system can be solved by various techniques: *closed form solutions* or *iterative solutons* based on either *linearization* or on *Kalman filtering*. As the time difference between the two stable local oscillators (ΔT) is a slow varying parameter it can easily be adapted for follow-up measurements.

In the second stage of the coherent signal processing in the navigation receiver unit, all results of the first stage are combined to determine the orientation of the receiver from the four distances $\mathbf{R_j} = [u_{xj}, u_{yj}, u_{zj}]$. The baseline between the points of origin on the two platforms can be calculated using

$$R = (|\mathbf{R_1}+\mathbf{R_{1r}}| + |\mathbf{R_2}+\mathbf{R_{2r}}| + |\mathbf{R_3}+\mathbf{R_{3r}}| + |\mathbf{R_4}+\mathbf{R_{4r}}|)/4$$

with $\mathbf{R_{jr}}$ the position vector of the navigation antenna ($j = 1,2,3,4$) on the receiver platform. $\mathbf{R_{jr}}$ is defined by the Cartesian coordinate system with the point of origin on the RX platform. By averaging over the four acquired baselines, the sensitivity against interferences and multipath effects is reduced.

The orientation between both platforms can be calculated from three of the four determined positions $\mathbf{R_j}$ of the navigation antennas on the RX platform.

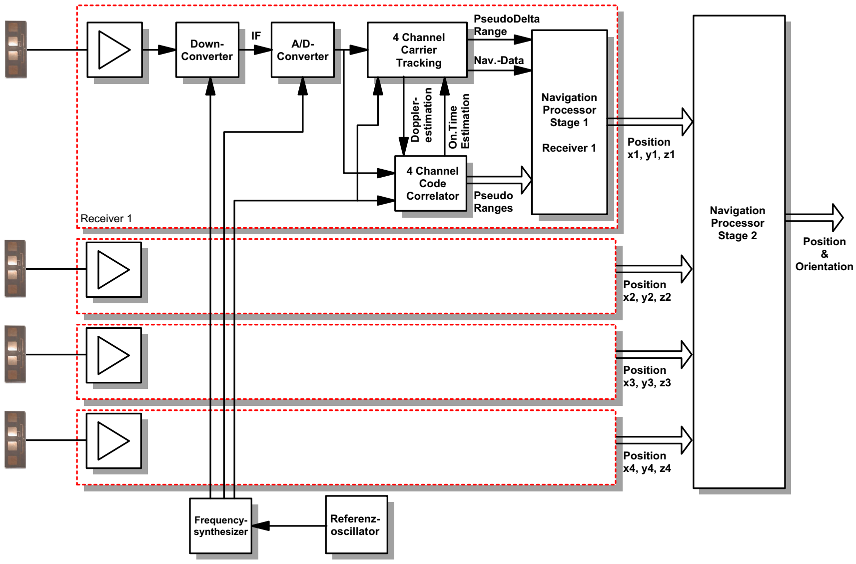

Figure 6: Block diagram of the navigation unit on the receiver platform

4 Carrier phase tracking

Using a monolithic navigation unit on the receiver side enables coherent signal processing over all four navigation receivers. Hence, a further enhancement of precise position and orientation estimation can be achieved by phase tracking of the received carriers. For carrier phase tracking of binary phase shift keying signals the punctual code correlator will remove the complete code structure of the binary phase shift keying (BPSK) navigation signals. Using a Costas phase discriminator the standard formula for the phase measurement variance σ^2_{Ph} is [9]:

$$\sigma^2_{Ph} = \frac{c^2}{4\,\pi^2\,f^2_{RF}}\,\frac{B_{PLL}}{C/N_0}\left(1 + \frac{1}{2\,C/N_0\,T_D}\right) \tag{7}$$

which is a good approximation for a binary phase shift key signals.

In Fig. 7 is shown the pseudorange phase measurement accuracy as a function of the signal-to-noise ratio calculated from (7). It was used an *arctan* PLL with a tracking loop bandwidth of 18 Hz and a predetection integration time of 1 ms. The carrier phase could not be tracked for C/N_0 values below 32 dBHz and cycle slips occur.

The problem is that the navigation receiver cannot distinguish one cycle of a carrier from another. The receiver measures the fractional phase, and keeps track of changes to the phase. The initial phase is undetermined, or ambiguous, by an integer number of cycles N.

Converting the carrier phase into a distance by multiplying by the carrier wavelength, we get

$$\Phi_{ij} = \phi^r_{ij}(t) - \phi^t_{ij}(t) + N_j + \epsilon_{ij} + f_c\Delta T \tag{8}$$

$$R_{ij} = \frac{\Phi_{ij}}{2\,\pi}\,\lambda \tag{9}$$

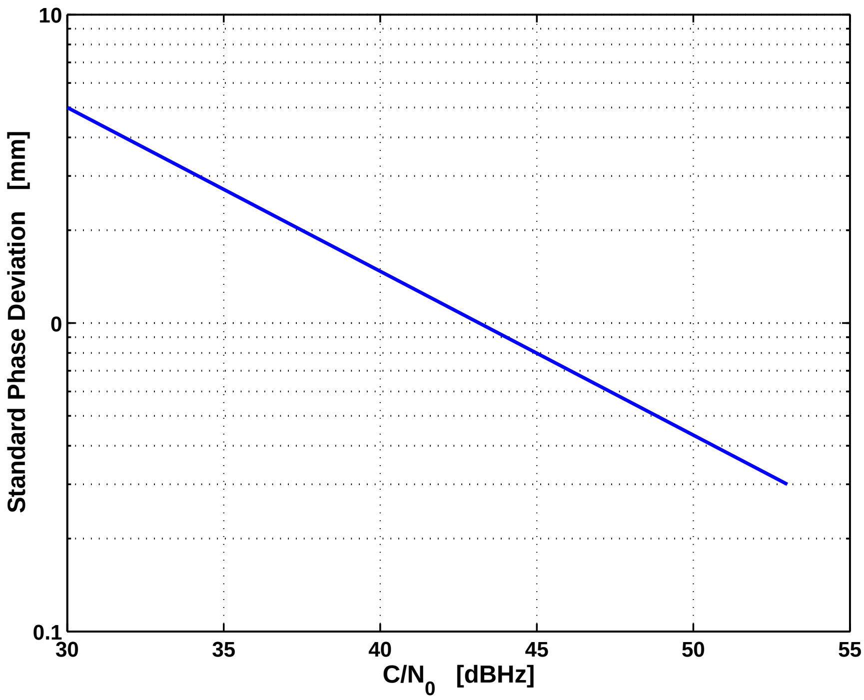

Figure 7: Pseudorange phase measurement accuracy plotted as a function of signal-to-noise ratio.

where Φ_{ij} is the length of propagation path between TX antenna i and receive antenna j in cycles, $\phi^r_{ij}(t)$ the received phase of navigation signal i at the receiver j at the time t, $\phi^t_{ij}(t)$ the transmitted phase of the navigation signal i is. The carrier frequency is f_c and the integer ambiguity term N_j. Multipath effects and receiver noise is taken into account by ϵ_{ij} and the time difference between transmitter and receiver is ΔT.

In comparison to GNSS all navigation signals are generated from a single stable oscillator. For that reason the coherent signal processing and phase tracking on the receiver platform yields an highly accurate position and orientation estimation.

5 Error estimation

Systematic errors (biases) and random noise affect the code pseudoranges R_{ij} and phase pseudoranges Φ_{ij}. The error sources can be classified into three groups (see Table 1).

In comparison to a GNSS the proposed method has less error sources. For instance the four navigation signals are derived from a single stable clock and they travel over a short distance of less than 100 km for airborne systems. Therefore the ionospheric and tropospheric refraction can be neglected, in contrast to any GNSS where the satellites are at an altitude of 20200 km. As the point of origin is on the transmit platform no prediction of the transmit position has to be performed, as it is the case for the position estimation of the satellites (ephemeris data).

Source	Effect
Transmitter	Clock and frequency stability Position errors
Signal propagation	Ionospheric refraction Tropospheric refraction
Receiver	Antenna phase center variation Receiver noise Resolution Clock bias Multipath

Table 1: Typical sources of range error in a global navigation satellite system

As mentioned earlier, the broadcast signals contain information about the actual position and motion of the TX platform and about the geometrical configuration of the TX navigation antennas. The data concerning position and motion may not exactly model the true platform motion, or the geometrical information about the TX antennas may not be exact. Distortion of the signal by measurement noise can further increase positional error (see Table 2).

Method	Estimated error
Code range	10-30cm
Phase range	0.2-5mm

Table 2: Estimated range error

Multipath effects, caused by bouncing off a reflective surface prior to reaching the RX-navigation antenna, are a serious concern. It is difficult to completely correct multipath errors. One has to ensure that the navigation antennas are mounted on places where multipath effects can be avoided. The antenna design has to take this effect into account to reduce the multipath error [7] [8].

6 Conclusion

A method is presented which allows determining baseline and orientation of two airborne platforms to each other. On the transmitter platform a navigation unit is installed. This unit generates four navigation signals from the stable local oscillator. Modulating each navigation signal with an individual PRN sequence allows using the same center frequency. Additional information, such as the position of the four navigation antennas on the TX platform and the absolut position of the transmitter, is also modulated on the navigation signal. On the receiver side the four navigation signals are received by four separate antennas and processed by a monolithic navigation unit. Due to this combination of four transmit and receive antennas and coherent signal processing of the navigation signals it is possible to determine the baseline and orientation of the platforms with high accuracy immediately.

References

[1] J.L. AUTERMAN: 'Phase stability requirements for bistatic SAR', IEEE National Radar Conference 1984, Atlanta, 13.-14. March, pp. 48-52

[2] M. WEISS: 'Synchronization of bistatic Radar systems', IEEE 2004 International Geoscience and Remote Sensing Symposium, Anchorage, Alaska, USA, pp. 1750-1753

[3] H. CANTALLOUBE, M. WENDLER, ET AL.: 'Challenges in SAR processing for airborne bistatic acquisitions', European conference on synthetic aperture radar (EUSAR 2004), Ulm, Germany, May 2004, pp. 577-580

[4] G. KRIEGER, H. FIEDLER, A. MOREIRA: 'Bi- and Multi-Static SAR: Potetials and Challenges', European conference on synthetic aperture radar (EUSAR 2004), Ulm, Germany, May 2004, pp. 365-370

[5] M. EINEDER: 'Oscillator clock drift compensation in bistatic interferometric SAR', IEEE 2003 International Geoscience and Remote Sensing Symposium, Toulouse, France, pp. 1449-1451

[6] M. WEISS: 'Time and Frequency Synchronization Aspects for Bistatic SAR Systems', European conference on synthetic aperture radar (EUSAR 2004), Ulm, Germany, May 2004, pp. 395-398

[7] R.B. LANGLEY: 'The GPS observables', GPS World, April, 1993

[8] R.B. LANGLEY: 'The GPS error budget', GPS World , 1997, Vol. 8, No. 3, pp. 51-56

[9] T. PANY, M. IRSIGLER, B. EISSFELLER, J. WINKEL; 'Code and Carrier Phase Tracking Performance of a Future Galileo RTK Receiver', Proceedings of the European Navigation Conference ENC-GNSS 2002, Copenhagen, 27-30 May 2002